











# Protective effects of quercetin against tongue injury and oxidative stress triggered by irinotecan: a histopathological, biochemical and molecular study

Eman Mohamed Faruk <sup>1,2</sup>, Fatma Ibrahim <sup>3,\*</sup>, Mahmoud M. Hassan <sup>4</sup>, Kamal M. Kamal <sup>5</sup>,  
Dina Allam Abdelmaksoud Hassan <sup>6</sup>, Ayat Abu-elnasr Awwad <sup>7</sup>, Neema Mahmoud Taha <sup>8</sup>,  
Mohamed Ghazy Attia Hablas <sup>9</sup>, Ahmed Mohammed Zaazaa <sup>10</sup>, Mai Hassan Ibrahim <sup>5</sup>

<sup>1</sup>Anatomy Department, College of Medicine, Umm Al-Qura University, Al Abidiyah, Makkah, Saudi Arabia,

<sup>2</sup>Department of Histology and Cell Biology, Faculty of Medicine, Benha University, Al Nadi Al Ryadi, Qism Benha 13518, Benha, Al-Qalyubia Governorate, Egypt,

<sup>3</sup>Department of Forensic Medicine and Clinical Toxicology, Faculty of Medicine, Zagazig University, Zagazig Rd inside Zagazig University, Shaibet an Nakareyah, Zagazig 44519, Al-Sharqia Governorate, Egypt,

<sup>4</sup>Department of Physiology, Faculty of Medicine, Benha University, Al Nadi Al Ryadi, Qism Benha, Al-Qalyubia Governorate, Benha 13518, Benha, Egypt,

<sup>5</sup>Department of Anatomy and Embryology, Faculty of Medicine, Benha University, Al Nadi Al Ryadi, Qism Benha, Al-Qalyubia Governorate, Benha 13518, Benha, Egypt,

<sup>6</sup>Department of Histology and Cell Biology, Faculty of medicine for girls, Al-Azhar University, Cairo 11651, Cairo, Egypt,

<sup>7</sup>Department of Otorhinolaryngology, Faculty of Medicine, Al-Azhar University, Cairo 11751, Cairo, Egypt,

<sup>8</sup>Department of Physiology, Umm Al-Qura University, Al Abidiyah, Makkah, Saudi Arabia,

<sup>9</sup>Department of Histology and Cell biology, faculty of medicine, Suez University, Suez 43221, Suez, Egypt,

<sup>10</sup>Student at Faculty of Medicine, Benha National University, Benha Colleges in Cairo, Main Axis of El-Obour City, Egypt

\*Corresponding author: Faculty of Medicine, Department of Forensic Medicine and Clinical Toxicology, Zagazig University, Zip code: 44519 Zagazig, Egypt.

Email: FISptan@medicine.zu.edu.eg, drfatmaibrahim88@gmail.com

**Introduction:** About 80% of patients receiving chemotherapeutics suffer from side effects related to the gastrointestinal tract. Irinotecan (CPT-11) is a chemotherapeutic agent usually used in treating solid tumors. Quercetin (QRT), a bioflavonoid, is an antioxidant and scavenger reactive oxygen species scavenger.

**Objective:** The current study explored the possible protective effects of QRT against mucosal tongue injury caused by CPT-11.

**Methods:** The study included four equal groups: group 1/control, group 2/QRT, group 3/CPT-11, and group 4/CPT-11 + QRT.

**Results:** CPT-11-induced tongue injury in the form of non-healed ulcers, absent lingual papillae, mononuclear cells infiltration, marked deposition of collagen fibers, and overexpression of CD86 and tumor necrosis factor- $\alpha$  (TNF- $\alpha$ ). The increased malondialdehyde levels, decreased superoxide dismutase and total antioxidant capacity revealed that there was an oxidative stress. Also, there was a decreased countenance of Ki-67 and Bcl-2 and an increased countenance of NF- $\kappa$ B. The QRT-treated group showed complete ulcer healing, with histological features almost like the control group, along with minimal collagen fiber deposition, decreased reactivity to CD86 and TNF- $\alpha$  and improvement of oxidative stress status and the molecular study results as well.

**Conclusion:** QRT possess protective properties against CPT-11-triggered tongue injury.

**Keywords:** CPT-11; Flavonoids; Oxidative stress; Malondialdehyde; CD86.

## 1 Introduction

Chemotherapy is effective against malignant cells and hindering the cancerous cells' spread and metastasis, however, patients receiving chemotherapy may have a number of side effects.<sup>1</sup> About 80% of malignancy-treated patients with chemotherapeutic agents suffer from side effects related to the gastrointestinal tract (GIT), including mucositis, nausea, vomiting, heartburn, stomachache, indigestion, and diarrhea.<sup>2,3</sup>

Irinotecan (CPT-11) is one of the semisynthetic plant alkaloid camptothecin products.<sup>4</sup> It is one of the inhibitors of topoisomerase I, which is usually used in cancers, such as colon, rectum, pancreas, and lung.<sup>5</sup>

Irinotecan is catalyzed by hydrolysis to two isoforms of carboxylesterases enzyme (CES1 and CES2) with subsequent production of the active metabolite 7-ethyl-10-hydroxy camptothecin

(SN38).<sup>6</sup> SN38 causes DNA cleavage and prevents the following ligation by blocking the enzyme on DNA, producing cytotoxic protein-linked DNA breaks with eventual cell death.<sup>7</sup>

Quercetin (3,3',4',5,7-Pentahydroxyflavone) is a bioflavonoid, which has a polyphenolic structure.<sup>8</sup> Fruits, vegetables, and seeds are rich sources of quercetin.<sup>9</sup>

Several experimental studies have stated the beneficial potentials of quercetin as anti-inflammatory,<sup>10</sup> antioxidant,<sup>11</sup> anti-cancer,<sup>12</sup> anti-hyperlipidemic,<sup>13</sup> anti-cytotoxic<sup>14</sup> and anti-ischemic.<sup>15</sup>

Quercetin has shown promising protective effects against toxicities induced by chemotherapeutic agents, involving various organs and tissues e.g.; cisplatin,<sup>16</sup> doxorubicin,<sup>17</sup> 5-fluorouracil<sup>18</sup> and cyclophosphamide.<sup>19</sup>

Quercetin can scavenge reactive nitrogen species as well as reactive oxygen species (ROS).<sup>20</sup> It is a chelator for iron and

calcium. It inhibits lipid peroxidation and modifies antioxidant defensive pathways *in vivo* and *in vitro*.<sup>20,21</sup>

In the current study, we examined the potential protective effects of quercetin against mucosal tongue injury caused by irinotecan.

## 2 Materials and methods

### 2.1 Chemicals

Irinotecan (CPT-11) and quercetin (QRT), as a yellow powder, were purchased from Sigma Chemical Co.

### 2.2 Experimental animals and study design

The study included 32 adult male albino rats (180–200 gm). Before starting the research, all rats were exposed to a period of passive acclimatization to be habituated to their surroundings, to ensure their physical health, and to omit any unhealthy animals. The Institutional Animal Care and Use Committee (IACUC) at Zagazig University consented to this study: (The approval number ZU-IACUC/3/F/302/2023).

Four equal tested groups were incorporated in this study, with eight rats for each. Group 1/control: received tap water and regular food.

Group 2/ Quercetin (QRT- treated group): received 100 mg/kg in 2 mL saline orally by gavage daily for 5 days. The dose was selected depending on the best results obtained by Singh et al.<sup>22</sup>

Group 3/ Irinotecan (CPT-11- treated group): received 200 mg/kg of CPT-11 in a sorbitol/lactic acid buffer as a single intraperitoneal (IP) injection in the first day of the experiment.<sup>23,24</sup>

Group 4/ Irinotecan+Quercetin (CPT-11 + QRT-treated group): received IP injection of CPT-11 (like group 3) and QRT (like group 2) for five days.

Upon completion of the experiment, (one day after the last dose of QRT), animals were anesthetized using 30 mg/kg IP sodium pentobarbital,<sup>25</sup> then rats were sacrificed by cervical dislocation.

### 2.3 Histological procedure and immunohistochemistry (IHC)

#### 2.3.1 Light microscopy

Tongue samples were dissected from the mouth at their base. Following this, tongue tissue was taken, preserved in 10% formalin solution, to be prepared into paraffin blocks. Then were sliced into sections measuring 3–5  $\mu\text{m}$  thick using a rotary microtome (LEICA RM 1215; UK). The sections underwent staining by hematoxylin & eosin (H&E) for standard histological analysis. Also, Mallory trichrome (MT) staining was done to show collagen fibers.<sup>26</sup> The slides were scrutinized and histomorphometric dimensions were conducted using a light microscope (Olympus-Bx; 4,500) paired with an ordinal camera (Nikon-Coolpix; 4,500). The objective lens magnifications were adjusted to  $\times 10$  and  $\times 40$  for analysis.

#### 2.3.2 Immunohistochemical detection of CD86 and TNF- $\alpha$ in tongue tissue sections:

Sections of the tongue were affixed onto positively charged glass slides and subjected to an immunohistochemical assay following the protocol outlined by Kiernan (2015)<sup>27</sup>. The primary antibody targeting CD86 and TNF- $\alpha$  was rabbit polyclonal antibodies sourced from AB Clonal Inc., Woburn, MA, USA (catalog #: A2353, A11534, respectively).

Using citrate buffer (Thermo Fisher Scientific, Eprelia, catalog #: AP9003–125) after deparaffinization and rehydration, antigens were extracted from the sections by boiling at pH 6 for 10 min. By incubating slides with an H<sub>2</sub>O<sub>2</sub> solution for 15 min, endogenous

peroxidase activity was blocked. A secondary antibody was then incubated overnight at 4 °C on the sections after the sections had been blocked with the corresponding protein. After each incubation step, PBS was used to wash the samples.

This immunoreaction was completed with TP-015-HD of the Lab Vision™ system from Thermo Fisher Scientific, which detects rabbit-specific polyvalent HRP/DAB. We visualized the stained cells using 3,3-diaminobenzidine (DAB) chromogen and counterstained with hematoxylin. The presence of CD86 and TNF- $\alpha$  immunopositivity was indicated by brownish cytoplasmic staining.

Negative control slides were prepared by omitting the primary antibody step. Slide assessment and photos were conducted using a Nikon Eclipse 80i microscope equipped with a TouPCam™ Xcam full HD camera. This process was carried out in the Department of Anatomy and Embryology, Faculty of Medicine, Benha University, Egypt.

#### 2.3.3 Histomorphometry

Histomorphometric analyses were conducted using the Image-Pro Plus software (version 6.0; Media Cybernetics Inc., Bethesda, Maryland, USA) at the Pathology Department, Faculty of Medicine, Benha University. The optical density of positive immunostaining for CD86 and TNF- $\alpha$  was assessed quantitatively. Five randomly selected high-power microscopic fields were assessed to determine the optical density.<sup>28,29</sup> Similarly, the percentage of area occupied by Mallory trichrome (MT)-stained collagen fibers was assessed at  $\times 20$  magnification.<sup>30</sup> The finding was presented as the mean area percentage of collagen per square micrometer ( $\mu\text{m}^2$ ).

### 2.4 Biochemical study of oxidative stress markers

For the tests, portions of the tongues were weighed and homogenized by adding nine times the volume of normal saline. The resulting 10% homogenate underwent centrifugation at 10,000 rpm for 15 min, after which the supernatant was diluted with ten times the volume of normal saline to achieve a 1% concentration. Tissue lysate was then stored at  $-80^\circ\text{C}$  for subsequent biochemical analysis.

The levels of malondialdehyde (MDA),<sup>31</sup> superoxide dismutase (SOD),<sup>32</sup> and total antioxidant capacity (TAC)<sup>33</sup> were determined colorimetrically by the manufacturer's instructions provided by Biodiagnostic Co, Egypt.

### 2.5 Molecular study (gene expression of ki-67, Bcl-2 and NF- $\kappa\text{B}$ )

#### 1) Total RNA Extraction from the Tongue Tissue

PeqLab Biotechnologie GmbH, Carl Thiersch St. 2B 91,052 Erlangen, Germany, Cat. No. 302010) was used to extract total RNA from tongue tissue according to manufacturer's instructions. RNA integrity and purity were measured using the UV spectrophotometer's absorbance at 260/280 nm.

### 2.6 Reverse transcription and cDNA synthesis

Utilizing the Maxima First Strand cDNA Synthesis Kit (Thermo Scientific, Waltham, MA, USA, cat #K1641), we reverse-transcribed the isolated RNA to synthesize complementary DNA (cDNA).

#### 1) Real-Time Polymerase Chain Reaction for mRNA Gene Expression

**Table 1.** The primer sequences of ki-67, Bcl-2 and NF- $\kappa$ B.

Genes	Primer Sequences (5' → 3')
Ki-67	F: 5'-ATTTTCAGTTCCGCCAATCC-3' R: 5'-GGCTTCCGTCTTCATACCTAAA-3'
Bcl-2	F: 5'-ATGCCTTTGTGGAAGTATATGGC-3' R: 5'-GGTATGCACCCAGAGTGATGC-3'
NF- $\kappa$ B	F: 5'-CTAGCTAGCTACGGCATCGATCG-3' R: 5'-CGTAGGAGTCGATCGATATAGCTACG-3'
GAPDH	F: 5'-AACTTTGGCATTGTGGAAGG-3' R: 5'-ACACATTGGGGGTAGGAACA-3'

Abbreviations: Ki-67, Antigen Kiel 67; *Nf- $\kappa$ b*, nuclear factor kappa B; Bcl-2, B-cell lymphoma 2; GAPDH, glyceraldehyde-3-phosphate dehydrogenase.

The expression levels of mRNA were determined using Real-Time PCR (Stratagene Mx3005P qPCR System). To normalize the data, GAPDH expression was used as a control. In this study, primer sequences are listed in Table 1. For each 25 L PCR reaction, 12.5 L TOPreal™ qPCR 2X PreMIX (SYBR Green with low ROX) (Cat. # RT500S or RT500M) (Enzynomics, Korea), 1 L primers (Invitrogen, USA), 5 L cDNA, and 5.5 L ddH<sub>2</sub>O were used. For the amplification process, 95 °C was used for 15 min of initial activation, followed by 40 cycles of denaturation at 94 °C for 15 seconds, annealing at 60 °C for 15 seconds, and elongation at 72 °C for 30 seconds. Expression of genes as a function of fold-change.

## 2.7 Statistical analysis

GraphPad Prism, Version 8.0 Software (GraphPad Software; San Diego, CA, USA) was used to compare the mean values and standard deviations of the studied groups. Statistical differences between groups were assessed using one-way ANOVA followed by post-hoc Bonferroni test. Significance was determined at a *P* value <0.05.

## 2.8 Histological findings

Comparing the effects of treatment between the control and QRT-treated groups on tongue tissue, sections stained with hematoxylin and eosin displayed uniformly distributed filiform papillae, consistent in extent, form, and alignment, along with a normal layer of keratinized epithelium covering the upper surface of the tongue. Additionally, well-developed connective tissue and muscles were observed. The lower surface appeared smooth without papillae (Fig. 1a–c). In contrast, the CPT-11-treated group exhibited non-healed ulcers with absent epithelial covering, adjacent to which lingual papillae were absent. Moreover, dilated blood vessels and mononuclear cells infiltrated the connective tissue in the ulcerated area (Fig. 1d). However, the CPT-11 + QRT-treated group showed complete ulcer healing, presenting histological features resembling those of the negative control group (Fig. 1e).

To evaluate collagen deposition, Mallory's trichrome stain was applied to tongue sections from all study groups. In the negative control and QRT-treated groups, collagen fibers were observed under epithelium and between muscle fibers (Fig. 2a and b). Conversely, the CPT-11-treated group exhibited significant collagen fiber accumulation under epithelium and related muscle fibers (Fig. 2c). Notably, the CPT-11 + QRT-treated group displayed minimal collagen fiber accumulation under epithelium and between muscle fibers, resembling that of the negative control group (Fig. 2d).

## 2.9 Immunohistochemical findings

The extent of the inflammatory response, tissue proliferation, and immunoreactivity of CD86 and TNF- $\alpha$  were examined. In the negative control and QRT-treated groups, the tongue exhibited a faint positive cytoplasmic reaction for CD86 in epithelial cells and a mild positive immune reaction for TNF- $\alpha$  in the stroma (Figs. 3a and b and 3e and f). Conversely, the CPT-11-treated group displayed a substantial positive cytoplasmic reaction for CD86 in epithelial cells and a strong positive immune reaction for TNF- $\alpha$  in the stroma (Figs. 3c and g). In contrast, the CPT-11 + QRT-treated group demonstrated faint positive cytoplasmic reactions for CD86 in epithelial cells and mild positive immune reactions for TNF- $\alpha$  in the stroma (Figs. 3d and h).

As shown in Fig. 4, the CPT-11 group had a considerably greater mean optical density of tongue epithelium CD86 than the negative control, QRT-treated group, and CPT-11 + QRT-treated group. Similar to this, as shown in Fig. 4, the mean optical density of TNF- $\alpha$  expression was significantly higher in the CPT-11 group compared to the negative control, QRT-treated group, and CPT-11 + QRT-treated group.

As illustrated in Fig. 5, the mean area percentage of collagen fiber disposition was also considerably larger in the CPT-11 group as compared to the QRT-treated group, the negative control, and the CPT-11 + QRT-treated group.

## 2.10 Biochemical findings

In the assessment of the oxidative stress markers, the study results revealed a significant increase in MDA levels in the CPT-11 group compared to the other groups (*P* < 0.001). Conversely, the levels of SOD and TAC showed a significant decrease in the CPT-11 group compared to the other groups, as illustrated in (Fig. 6a–c). In the CPT-11 + QRT-treated group, there was a decrease in MDA levels and an increase in SOD and TAC levels compared to the CPT-11 group, as shown in (Fig. 6a–c).

## 2.11 Molecular study results

Upon examination of the various groups, it was observed that the group treated with CPT-11 exhibited a noteworthy reduction in the molecular gene expression of Ki-67 and antiapoptotic Bcl-2 levels. Additionally, there was a substantial increase in the NF- $\kappa$ B mRNA gene expression level within this group, as shown in Fig. 7.

## 3 Discussion

Our results revealed that CPT-11 induced tongue injury in the form of non-healed ulcers, absent lingual papillae, dilated blood vessels, mononuclear cells infiltration, marked deposition of collagen fibers and overexpression of CD86 as well as TNF- $\alpha$ . Regarding the biochemical results, there was oxidative stress evidenced by raised MDA levels along with decreased SOD and TAC levels.

Chemotherapeutic agents, including CPT-11, affect the rapidly proliferating cells of the GIT and may produce stomatitis, cheilosis, glossitis, esophagitis, and oral ulceration.<sup>34</sup> The pathogenesis of CPT-11-induced oral toxic effects could be attributed to many factors. CPT-11 leads to disastrous breaks during the replication of the double-stranded DNA triggering apoptosis.<sup>35</sup>

In addition, CPT-11 causes triggering of the natural immune system by activating oxidative stress and liberation of ROS.<sup>36</sup> CPT-11 increases the creation and activation of pro-inflammatory cytokines such as TNF- $\alpha$  and NF- $\kappa$ B, which results in initiation of pro-apoptotic pathways.<sup>37,38</sup> The detrimental effect of inflammatory intermediaries directly or indirectly increases vascular



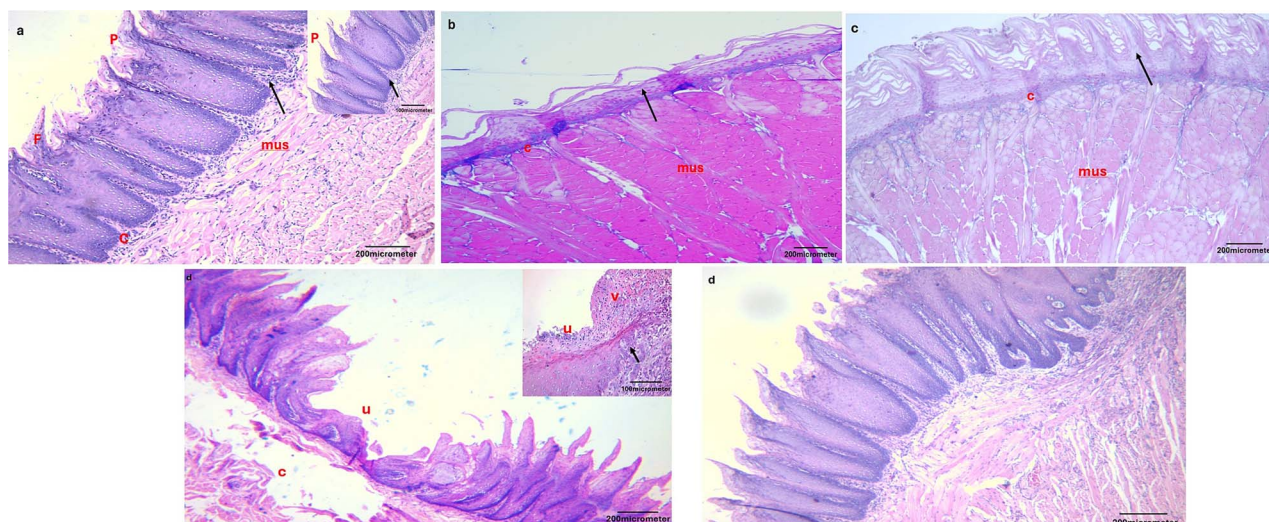


**Fig. 1.** a) A histological photo reveals the upper part of a rat's tongue from the control group, revealing neatly arranged, elongated conical filiform papillae with tapered ends (P). These papillae possess a connective tissue core beneath a layer of stratified epithelium (arrow). A fungiform papilla is visible (F), while the underlying surface epithelium comprises connective tissue (C). Notably, the tongue muscle cells exhibit diverse orientations (mus). (H&EX100). b) A histological photo of the lower surface of a rat's tongue from the control group depicts an absence of lingual papillae and the existence of a smooth keratin layer (arrow). The connective tissue forms the underlying lamina propria (c). The muscle fibers of the tongue are oriented in various directions (mus). (H&EX100). c) A histological photo displays the upper part of a rat's tongue from the QRT-treated group, depicting lingual papillae (arrow) alongside the underlying lamina propria (c). Furthermore, the lingual muscle fibers exhibit varying orientations (mus). (H&EX100). d) A histological photo of the upper surface of a rat's tongue from the CPT-11-treated group, revealing a noticeable ulcer (u) devoid of epithelial covering. Closest to the ulcer, the epithelial covering lacks lingual papillae. Notably, the lamina propria exhibits disorganized connective tissue fibers (c). (H&EX100). At higher magnification of the preceding section, an evident ulcer (u) is visible without epithelial covering. Within the lamina propria, there is pronounced infiltration of mononuclear cells (arrow) alongside numerous cell vacuolations (V). (H&EX200). e) A histological photo capturing the upper part of a rat's tongue from the CPT-11 + QRT-treated group reveals full epithelial covering and closely resembles that of the normal tissue. (H&EX100).

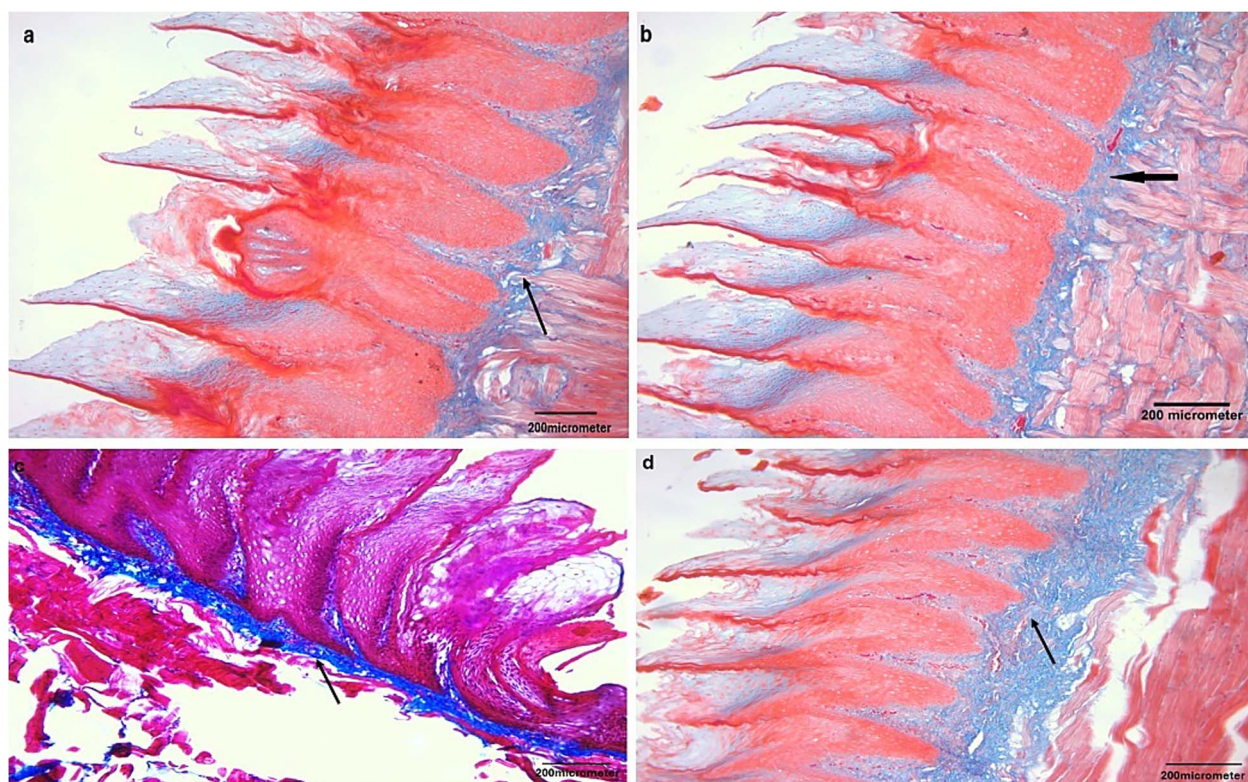


**Fig. 2.** a) A histological photo of the upper part of the rat's tongue from the first group reveals collagen fiber accumulation (arrow) within the lamina propria and amidst the muscle fibers, the collagen fibers exhibit a blue hue. b) A histological photo of the upper surface of the rat's tongue from the QRT-treated group reveals collagen fiber deposition (arrow) within the lamina propria and interspersed among the muscle fibers. c) A histological photo of the upper surface of a rat's tongue from the CPT-11-treated group reveals an increase in collagen fiber deposition (arrow) within the lamina propria and among the muscle fibers. d) A histological photo of the upper surface of the rat's tongue CPT-11 + QRT-treated group reveals a reduction in collagen fiber accumulation (arrow) underlying epithelium and among the muscle cells. (Mallory trichrome X100).



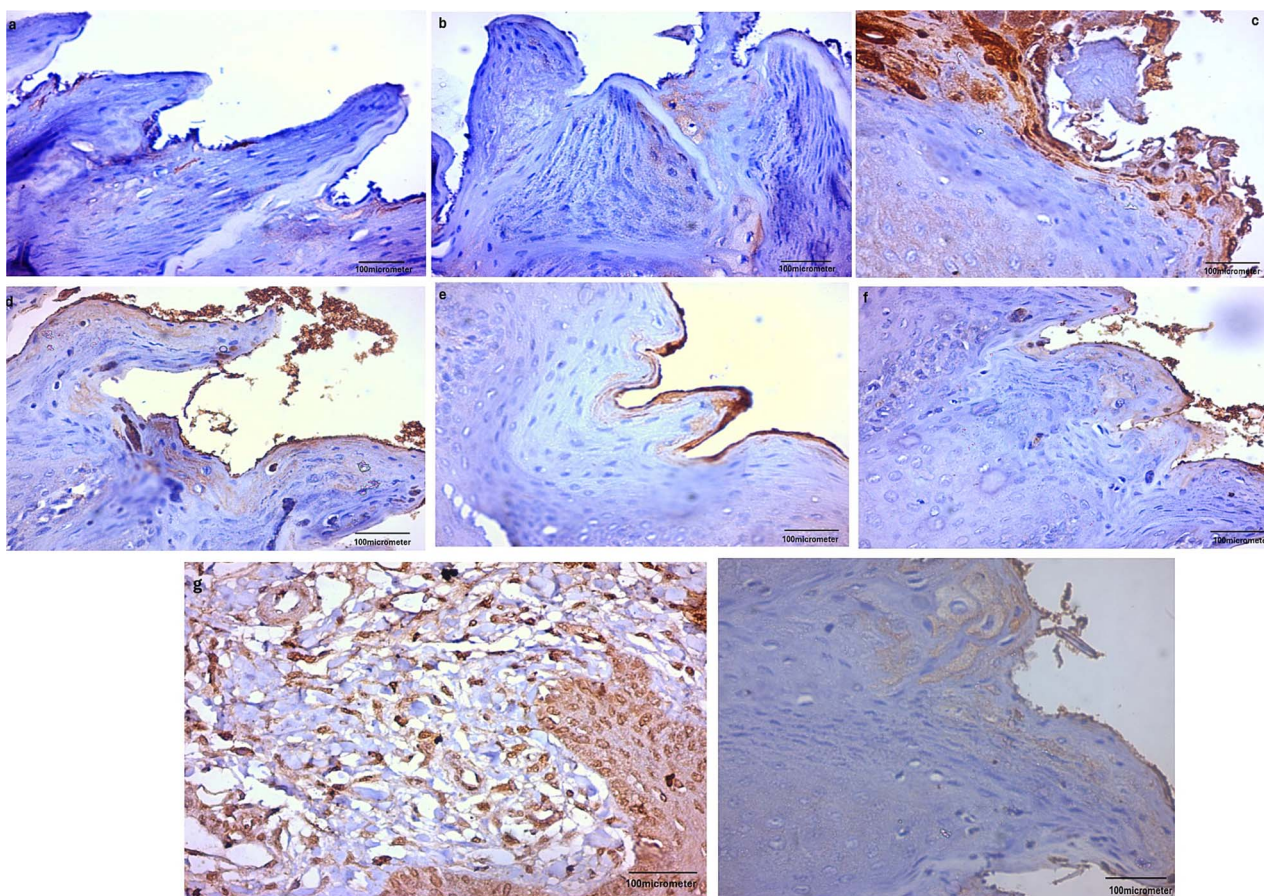


**Fig. 3.** a) A histological photo of the upper part of a rat's tongue from the control group reveals a weak positive cytoplasmic reaction for CD86 in the surface cells. b): A histological photo of the upper surface of a rat's tongue from the QRT-treated group reveals a weak positive cytoplasmic reaction for CD 86 in the epithelial cells. c): A histological photo of the upper part of a rat's tongue from the CPT-11-treated group reveals a strong positive cytoplasmic reaction for CD86 in the epithelial cells. d): A histological photo of the upper surface of a rat's tongue from the CPT-11 + QRT-treated group reveals a weak positive cytoplasmic reaction (arrow) for CD86 in the epithelial cells. (Avidine biotin peroxidase stain with Hx counter stain X 200). e): A histological photo of the upper part of a tongue of rat's tongue from the control group reveals an uncertain positive immune reaction for TNF- $\alpha$ . f): A histological photo of the upper surface of a rat's tongue from the QRT-treated group reveals a weak positive immune reaction for TNF- $\alpha$ . g): A histological photo of the upper part of the tongue of a rat's tongue from the CPT-11-treated group reveals a strong positive immune reaction for TNF- $\alpha$ . h): A histological photo of the upper surface of a rat's tongue from the CPT-11 + QRT-treated group reveals a weak positive immune reaction for TNF- $\alpha$ . (Avidine biotin peroxidase stain with Hx counter stain X200).

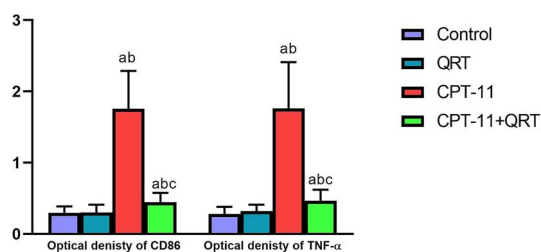


**Fig. 4.** Effects of QRT and CPT-11 on the optical density of CD86 and TNF- $\alpha$ . each quantity is mean  $\pm$  SD for 8 rats in each group. <sup>a</sup> Significant vs control, <sup>b</sup>significant vs QRT, <sup>c</sup>significant vs CPT-11. Abbreviations: TNF- $\alpha$ : Tumor necrosis factor- alpha, QRT: Quercetin, CPT-11: Irinotecan.

absorbency with further absorption of the drug into the oral mucosa.<sup>39</sup>

Formation of MDA can be induced non-enzymatically by ROS or enzymatically by the activity of lipoxygenase.<sup>40</sup> The assessment of MDA levels in various biological systems can be used as a significant parameter of lipid peroxidation both in vitro and in vivo. Throughout the process of intracellular oxidative stress,

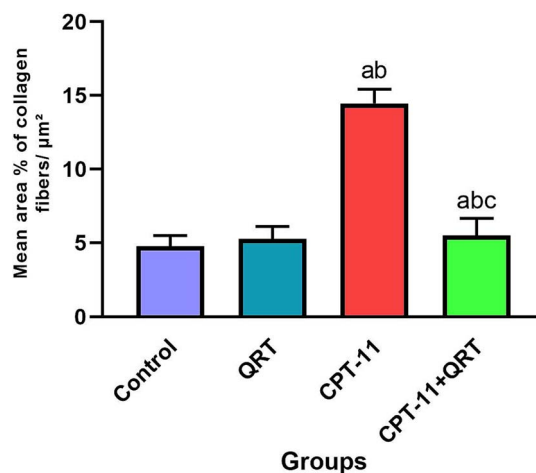


**Fig. 5.** Effects of QRT and CPT-11 on the mean area percentage of collagen per square micrometer ( $\mu\text{m}^2$ ). Each value is mean  $\pm$  SD for 8 rats in each group. <sup>a</sup> Significant vs control, <sup>b</sup>significant vs QRT, <sup>c</sup>significant vs CPT-11. Abbreviations: QRT: Quercetin, CPT-11: Irinotecan.

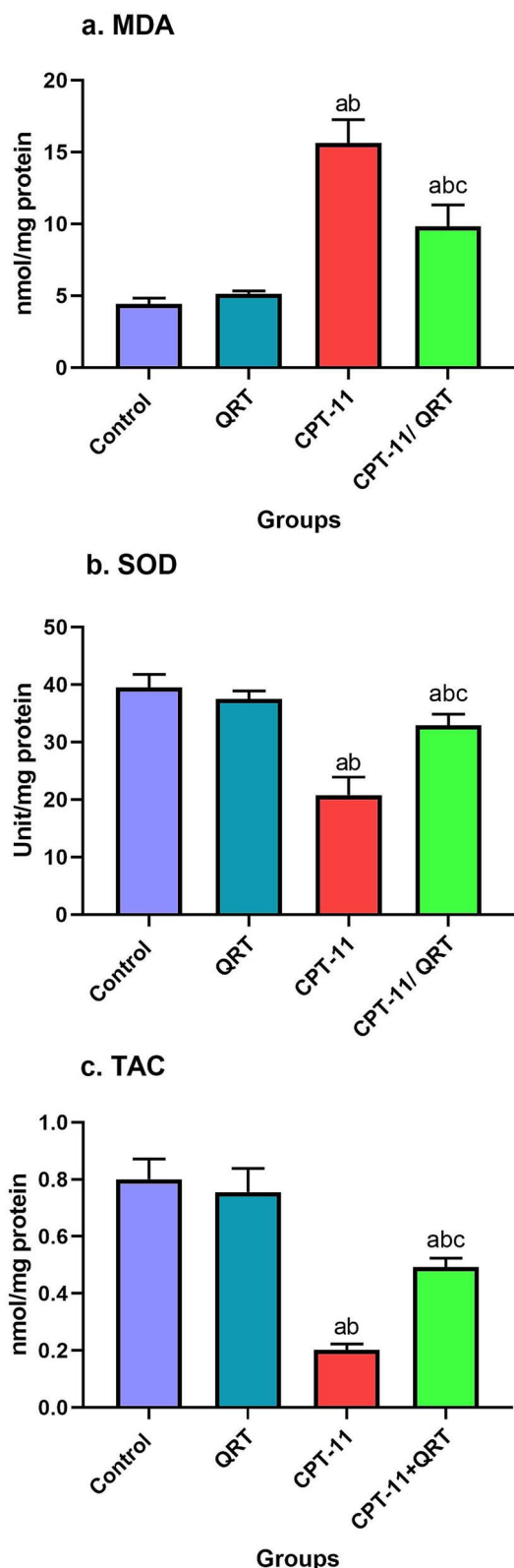


**Fig. 6.** Effects of QRT and CPT-11 on the biochemical parameters. Each value is mean  $\pm$  SD for 8 rats in each group. <sup>a</sup> Significant vs control, <sup>b</sup>significant vs QRT, <sup>c</sup>significant vs CPT-11. Abbreviations: MDA: Malondialdehyde, SOD: Superoxide dismutase, TAC: Total antioxidant capacity, QRT: Quercetin, CPT-11: Irinotecan.

**Gene Expression of ki-67, Bcl-2 and NF- $\kappa$ B**

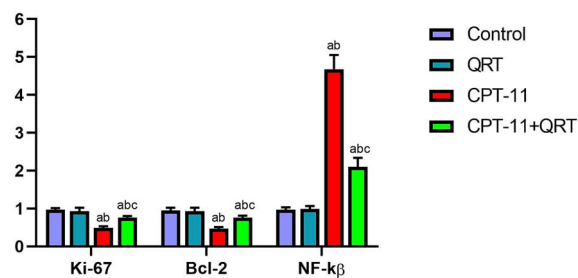


**Fig. 7.** Effects of QRT and CPT-11 on the gene expression of ki67, Bcl-2 and NF- $\kappa$ B. Each value is mean  $\pm$  SD for 8 rats in each group. <sup>a</sup> Significant vs control, <sup>b</sup>significant vs QRT, <sup>c</sup>significant vs CPT-11. Abbreviations: QRT: Quercetin, CPT-11: Irinotecan.

MDA reacts with DNA-forming adducts which marks it as a main factor in the damage to DNA.<sup>41</sup>

Superoxide dismutase is a corner stone in the physiological antioxidant defense strategy inside the cell, both in mammals and plants. It is effective versus free radicals and ROS produced from biotic and abiotic stress.<sup>42,43</sup>

Assessment of the TAC is one of the approaches that is most commonly used to evaluate the oxidant-antioxidant imbalance in the biological systems.<sup>44</sup> It has the importance of being a method to estimate the antioxidant capability of whole antioxidants in a natural sample and not only a sole item.<sup>45</sup>

Oral mucositis is one of the well-known, painful and devastating consequences of chemotherapy and radiotherapy.<sup>46</sup> It is defined as erythematous and hyperemic changes of the oral mucosa, boundaries of the tongue, base of the mouth, and/or soft palate that may advance into small abrasions or deep and painful ulcerations with bleeding, leading to poor appetite, dysphagia, enlarged risk of multiple infections and discontinuation of the therapy sessions.<sup>47,48</sup>

Upon analyzing the current study, our findings align with previous research,<sup>49–52</sup> indicating that CPT-11 induces direct DNA damage and activates the innate immune response through oxidative stress, leading to ROS release and heightened levels of inflammatory cytokines. Our study also revealed reduced expression of Ki-67 and Bcl-2, accompanied by increased NF- $\kappa$ B expression in the CPT-11-treated group at the mRNA level as determined by qRT-PCR.

Ki-67 serves as a nuclear antigen associated with cell proliferation during various phases of the cell cycle,<sup>53</sup> playing a crucial role in the formation of the ribonucleoprotein sheath around condensed chromosomes and the prevention of chromosomal aggregation.<sup>54</sup>

The Bcl-2 gene encodes proteins and is present in the nuclear membrane, inner mitochondrial surface, and endoplasmic reticulum. It plays a vital role in inhibiting apoptosis and preserving cell survival.<sup>55</sup> The meticulous mechanism by which Bcl-2 obstructs apoptosis is still indefinite, it was proposed that Bcl-2 may suppress mitochondrial cytochrome c translocation and concurrently inhibit caspase activation.<sup>56</sup>

Nuclear factor-kappa B (NF- $\kappa$ B) is an essential transcription factor that adjusts numerous functions inside cells, for instance, modification of inflammatory reactions, as well as control of some processes that are linked to cell survival or apoptosis.<sup>57</sup> In recent times, there has been a surge in studies aimed at delving into the pathogenesis of mucositis and its potential association with the NF- $\kappa$ B signaling pathway.<sup>58</sup> The oxidative stress resulted

from chemotherapeutics and CPT-11 as well, is an important factor in the pathogenesis of oral mucositis, so many antioxidants have been used either in the prophylaxis or even the treatment of oral mucositis.<sup>59</sup>

Our results revealed that QRT-treated group showed complete ulcer healing, with histological features almost like the control group, along with minimal collagen fiber deposition, decreased reactivity to CD86 and TNF- $\alpha$  and improvement of oxidative stress status.

In accord with our results, study of Lotfi et al.<sup>60</sup> has stated that QRT was efficient not only in preventing the tissue damage occurring in oral mucositis, but also can counteract the oxidative stress and cell apoptosis. The protective effect of QRT could be defended by its ability to conserve the proliferative activity and lessening of apoptotic changes of the basal epithelial cells of the oral mucosa.<sup>61</sup>

Also, previous studies<sup>62–64</sup> have reported the efficacy of QRT in relieving the oxidative stress status represented by decreased MDA levels and increased levels of SOD and TAC. Quercetin can inhibit the expression CD86 and TNF- $\alpha$ ,<sup>65</sup> which also supports our results.

In this study, QRT treatment caused increased appearance of Ki-67 and Bcl-2 and decreased appearance of NF- $\kappa$ B, which matches formerly-reported results.<sup>66,67</sup>

## 4 Conclusion

The results of this study revealed that CPT-11 induced evident damage in the tongues of adult albino rats, as determined by histopathological and biochemical results. Quercetin minimized this damage when it was co-administrated with CPT-11.

## Author contributions

All authors contributed equally to conceptualisation, methodology and writing (original draft, review and editing). All authors read and approved the final manuscript.

## Funding

The authors have no sources of funding to declare.

*Conflict of interest statement:* There are no conflicts of interest.

## Data availability

Data will be available from the corresponding author on reasonable request.

## References

- Smith P, Lavery A, Turkington RC. An overview of acute gastrointestinal side effects of systemic anti-cancer therapy and their management. *Best Pract Res Clin Gastroenterol*. 2020;48:101691.
- Keefe DM. Gastrointestinal mucositis: a new biological model. *Support Care Cancer*. 2004;12(1):6–9.
- Secombe KR, Collier JK, Gibson RJ, Wardill HR, Bowen JM. The bidirectional interaction of the gut microbiome and the innate immune system: implications for chemotherapy-induced gastrointestinal toxicity. *Int J Cancer*. 2019;144(10):2365–2376.
- Fuchs C, Mitchell EP, Hoff PM. Irinotecan in the treatment of colorectal cancer. *Cancer Treat Rev*. 2006;32(7):491–503.
- de Man FM, Goey AK, van Schaik RH, Mathijssen RHJ, Bins S. Individualization of irinotecan treatment: a review of pharmacokinetics, pharmacodynamics, and pharmacogenetics. *Clin Pharmacokinet*. 2018;57(10):1229–1254.
- Santos A, Zanetta S, Cresteil T, Deroussent A, Pein F, Raymond E, Vernillet L, Risse ML, Boige V, Gouyette A, et al. Metabolism of irinotecan (CPT-11) by CYP3A4 and CYP3A5 in humans. *Clin Cancer Res*. 2000;6(5):2012–2020.
- Bailly C. Irinotecan: 25 years of cancer treatment. *Pharmacol Res*. 2019;148:104398.
- İkizler M, Erkasap N, Dernek S, et al. Dietary polyphenol quercetin protects rat hearts during reperfusion: enhanced antioxidant capacity with chronic treatment. *Anadolu Kardiyol Derg*. 2007;7(4):404–410.
- Rezaei-Sadabady R, Eidi A, Zarghami N, Barzegar A. Intracellular ROS protection efficiency and free radical-scavenging activity of quercetin and quercetin-encapsulated liposomes. *Artif Cells, Nanomed Biotechnol*. 2016;44(1):128–134.
- Hädrich G, Vaz GR, Maidana M, Kratz JM, Loch-Neckel G, Favarin DC, Rogerio AP, da Silva FMR Jr, Muccillo-Baisch AL, Dora CL. Anti-inflammatory effect and toxicology analysis of oral delivery quercetin nanosized emulsion in rats. *Pharm Res*. 2016;33(4):983–993.
- Şengül E, Gelen V, Gedikli S, Özkanlar S, Gür C, Çelebi F, Çınar A. The protective effect of quercetin on cyclophosphamide-induced lung toxicity in rats. *Biomed Pharmacother*. 2017;92:303–307.
- Tang S-M, Deng X-T, Zhou J, Li QP, Ge XX, Miao L. Pharmacological basis and new insights of quercetin action in respect to its anti-cancer effects. *Biomed Pharmacother*. 2020;121:109604.
- Gomes IB, Porto ML, Santos MC, Campagnaro BP, Gava AL, Meyrelles SS, Pereira TMC, Vasquez EC. The protective effects of oral low-dose quercetin on diabetic nephropathy in hypercholesterolemic mice. *Front Physiol*. 2015;6:247.
- Zhu X, Li N, Wang Y, Ding L, Chen H, Yu Y, Shi X. Protective effects of quercetin on UVB irradiation-induced cytotoxicity through ROS clearance in keratinocyte cells. *Oncol Rep*. 2017;37(1):209–218.
- Bartekova M, Radosinska J, Pancza D, Barancik M, Ravingerova T. Cardioprotective effects of quercetin against ischemia-reperfusion injury are age-dependent. *Physiol Res*. 2016;65:S101–S107.
- Najafi M, Tavakol S, Zarrabi A, Ashrafizadeh M. Dual role of quercetin in enhancing the efficacy of cisplatin in chemotherapy and protection against its side effects: a review. *Arch Physiol Biochem*. 2022;128(6):1438–1452.
- Li S, Yuan S, Zhao Q, Wang B, Wang X, Li K. Quercetin enhances chemotherapeutic effect of doxorubicin against human breast cancer cells while reducing toxic side effects of it. *Biomed Pharmacother*. 2018;100:441–447.
- Lotfi M, Kazemi S, Shirafkan F, Hosseinzadeh R, Ebrahimpour A, Barary M, Sio TT, Hosseini SM, Moghadamnia AA. The protective effects of quercetin nano-emulsion on intestinal mucositis induced by 5-fluorouracil in mice. *Biochem Biophys Res Commun*. 2021;585:75–81.
- Kocahan S, Dogan Z, Erdemli E, Taskin E. Protective effect of quercetin against oxidative stress-induced toxicity associated with doxorubicin and cyclophosphamide in rat kidney and liver tissue. *Iran J Kidney Dis*. 2017;11(2):124–131.
- Mira L, Tereza Fernandez M, Santos M, Rocha R, Helena Florêncio M, Jennings KR. Interactions of flavonoids with iron and copper ions: a mechanism for their antioxidant activity. *Free Radic Res*. 2002;36(11):1199–1208.



21. Coldiron AD Jr, Sanders RA, Watkins JB III. Effects of combined quercetin and coenzyme Q10 treatment on oxidative stress in normal and diabetic rats. *J Biochem Mol Toxicol*. 2002;16(4):197–202.
22. Singh DP, Borse SP, Nivsarkar M. Overcoming the exacerbating effects of ranitidine on NSAID-induced small intestinal toxicity with quercetin: providing a complete GI solution. *Chem Biol Interact*. 2017;272:53–64.
23. al-Dasooqi N, Gibson RJ, Bowen JM, Logan RM, Stringer AM, Keefe DM. Matrix metalloproteinases are possible mediators for the development of alimentary tract mucositis in the dark agouti rat. *Exp Biol Med*. 2010;235(10):1244–1256.
24. al-Ansari S, Jalali R, Bronckers T, Raber-Durlacher J, Logan R, de Lange J, Rozema F. The effect of a single injection of irinotecan on the development of enamel in the Wistar rats. *J Cell Mol Med*. 2018;22(3):1501–1506.
25. Karthikeyan M, Arunakaran J, Balasubramanian K. The effects of prolactin and corticosterone on insulin binding to rat Leydig cells. *Reprod Biol*. 2009;9(2):189–194.
26. Bancroft JD, Layton C, Suvana SK. *Bancroft's theory and practice of histological techniques*. Churchill Livingstone Elsevier; Amsterdam, The Netherlands, 2013
27. Kiernan J. *Histological and histochemical methods*. Scion publishing ltd; The Old Hayloft, Vantage Business Park, Bloxham Road, Banbury, OX16 9UX, UK. 2015.
28. Zhao R, Guan D-W, Zhang W, du Y, Xiong CY, Zhu BL, Zhang JJ. Increased expressions and activations of apoptosis-related factors in cell signaling during incised skin wound healing in mice: a preliminary study for forensic wound age estimation. *Legal Med*. 2009;11:S155–S160.
29. Zhuang P-Y, Shen J, Zhu X-D, Lu L, Wang L, Tang ZY, Sun HC. Prognostic roles of cross-talk between peritumoral hepatocytes and stromal cells in hepatocellular carcinoma involving peritumoral VEGF-C, VEGFR-1 and VEGFR-3. *PLoS One*. 2013;8(5):e64598.
30. Benzie IF, Strain JJ. The ferric reducing ability of plasma (FRAP) as a measure of “antioxidant power”: the FRAP assay. *Anal Biochem*. 1996;239(1):70–76.
31. Ohkawa H, Ohishi N, Yagi K. Assay for lipid peroxides in animal tissues by thiobarbituric acid reaction. *Anal Biochem*. 1979;95(2):351–358.
32. Nishikimi M, Roa N, Yogi K. Determination of superoxide dismutase in tissue homogenate. *Biochem Bioph Res Commun*. 1972;46(2):849–854.
33. Koracevic D, Koracevic G, Djordjevic V, Andrejevic S, Cosic V. Method for the measurement of antioxidant activity in human fluids. *J Clin Pathol*. 2001;54(5):356–361.
34. Mitchell EP, editor. *Gastrointestinal toxicity of chemotherapeutic agents*. *Seminars in oncology*. Elsevier, WB Saunders. 2006;33(1):106–120.
35. Wang Y, Wei B, Wang D, Wu J, Gao J, Zhong H, Sun Y, Xu Q, Liu W, Gu Y, et al. DNA damage repair promotion in colonic epithelial cells by andrographolide downregulated cGAS–STING pathway activation and contributed to the relief of CPT-11-induced intestinal mucositis. *Acta Pharm Sin B*. 2022;12(1):262–273.
36. Gibson RJ, Bowen JM, Alvarez E, Finnie J, Keefe DMK. Establishment of a single-dose irinotecan model of gastrointestinal mucositis. *Chemotherapy*. 2007;53(5):360–369.
37. Goto S, Okutomi T, Suma Y, Kera J, Soma G, Takeuchi S. Induction of tumor necrosis factor by a camptothecin derivative, irinotecan, in mice and human mononuclear cells. *Anticancer Res*. 1996;16(5A):2507–2511.
38. Logan RM, Stringer AM, Bowen JM, Yeoh ASJ, Gibson RJ, Sonis ST, Keefe DMK. The role of pro-inflammatory cytokines in cancer treatment-induced alimentary tract mucositis: pathobiology, animal models and cytotoxic drugs. *Cancer Treat Rev*. 2007;33(5):448–460.
39. Saso L, Suzen S, Borges F, Csont T. Chemistry and pharmacology of modulators of oxidative stress. *Curr Med Chem*. 2020;27(13):2038–2039.
40. Farmer EE, Mueller MJ. ROS-mediated lipid peroxidation and RES-activated signaling. *Annu Rev Plant Biol*. 2013;64(1):429–450.
41. Zhang Y, Chen S-Y, Hsu T, Santella RM. Immunohistochemical detection of malondialdehyde–DNA adducts in human oral mucosa cells. *Carcinogenesis*. 2002;23(1):207–211.
42. Miller A-F. Superoxide dismutases: ancient enzymes and new insights. *FEBS Lett*. 2012;586(5):585–595.
43. Stephenie S, Chang YP, Gnanasekaran A, Esa NM, Gnanaraj C. An insight on superoxide dismutase (SOD) from plants for mammalian health enhancement. *J Funct Foods*. 2020;68:103917.
44. Fraga CG, Oteiza PI, Galleano M. In vitro measurements and interpretation of total antioxidant capacity. *Biochim Biophys Acta (BBA)-Gen Subj*. 2014;1840(2):931–934.
45. Kusano C, Ferrari B. Total antioxidant capacity: a biomarker in biomedical and nutritional studies. *J Cell Mol Biol*. 2008;7(1):1–15.
46. Worthington HV, Clarkson JE, Bryan G, Furness S, Glenney AM, Littlewood A, McCabe MG, Meyer S, Khalid T. Interventions for preventing oral mucositis for patients with cancer receiving treatment. *Cochrane Database Syst Rev*. 2011;(4):1–234.
47. Peterson D, Bensadoun R-J, Roila F. Management of oral and gastrointestinal mucositis: ESMO clinical practice guidelines. *Ann Oncol*. 2011;22(Suppl 6):vi78–vi84.
48. Jadaud E, Bensadoun RJ. Low-level laser therapy: a standard of supportive care for cancer therapy-induced oral mucositis in head and neck cancer patients? *Laser therapy*. 2012;21(4):297–303.
49. Ibrahim MAAH, Elwan WM. Effect of irinotecan on the tongue mucosa of juvenile male albino rat at adulthood. *Int J Exp Pathol*. 2019;100(4):244–252.
50. Wu Y, Wang D, Yang X, Fu C, Zou L, Zhang J. Traditional Chinese medicine Gegen Qinlian decoction ameliorates irinotecan chemotherapy-induced gut toxicity in mice. *Biomed Pharmacother*. 2019;109:2252–2261.
51. Arafat EA, el-khair SMA, Elsamanoudy A, Shabaan DA. Study of the possible alleviated role of atorvastatin on Irinotecan-induced lingual mucosal damage: histological and molecular study. *Oxidative Med Cell Longev*. 2021;2021(1):1–13.
52. Gençosman S, Ceylanlı D, Şehirli AÖ, Teralı K, Bölükbaşı F, Çetinel Ş, Sayiner S. Investigation of the possible protective effect of N-acetylcysteine (NAC) against irinotecan (CPT-11)-induced toxicity in rats. *Antioxidants*. 2022;11(11):2219.
53. Lazăr D, Tăban S, Sporea I, Dema A, Cornianu M, Lazăr E, Goldiş A, Vernic C. Ki-67 expression in gastric cancer. Results from a prospective study with long-term follow-up. *Romanian J Morphol Embryol*. 2010;51(4):655–661.
54. Sun X, Kaufman PD. Ki-67: more than a proliferation marker. *Chromosoma*. 2018;127(2):175–186.
55. Ribeiro DA, Salvadori DM, Marques ME. Abnormal expression of bcl-2 and bax in rat tongue mucosa during the development of squamous cell carcinoma induced by 4-nitroquinoline 1-oxide. *Int J Exp Pathol*. 2005;86(6):375–382.
56. Gogvadze V, Orrenius S, Zhivotovsky B. Multiple pathways of cytochrome c release from mitochondria in apoptosis. *Biochim Biophys Acta (BBA)-Bioenerg*. 2006;1757(5–6):639–647.



57. Oeckinghaus A, Ghosh S. The NF- $\kappa$ B family of transcription factors and its regulation. *Cold Spring Harb Perspect Biol.* 2009;1(4):a000034.
58. Abeesh P, Guruvayoorappan C. NF- $\kappa$ B as a potential target for the treatment and prevention of Mucositis. *Curr Pharm Biotechnol.* 2023;24(13):1613–1622.
59. Nguyen H, Sangha S, Pan M, Shin DH, Park H, Mohammed AI, Cirillo N. Oxidative stress and chemoradiation-induced oral mucositis: a scoping review of in vitro, in vivo and clinical studies. *Int J Mol Sci.* 2022;23(9):4863.
60. Lotfi M, Kazemi S, Ebrahimpour A, Shirafkan F, Pirzadeh M, Hosseini M, Moghadamnia AA. Protective effect of quercetin nanoemulsion on 5-fluorouracil-induced oral mucositis in mice. *J Oncol.* 2021;2021:1–10.
61. Zhang J, Hong Y, Liuyang Z, Li H, Jiang Z, Tao J, Liu H, Xie A, Feng Y, Dong X, et al. Quercetin prevents radiation-induced oral mucositis by upregulating BMI-1. *Oxidative Med Cell Longev.* 2021;2021(1):1–16.
62. Sedky A, Mahboub F, Elsayy H, Eid R. Protective potential of quercetin on Cd-induced hepatorenal damage. *Pol J Environ Stud.* 2017;26(5):2197–2205.
63. Wang J, Zhu H, Wang K, Yang Z, Liu Z. Protective effect of quercetin on rat testes against cadmium toxicity by alleviating oxidative stress and autophagy. *Environ Sci Pollut Res.* 2020;27(20):25278–25286.
64. Baran M, Yay A, onder GO, canturk Tan F, Yalcin B, Balcioglu E, Yildiz OG. Hepatotoxicity and renal toxicity induced by radiation and the protective effect of quercetin in male albino rats. *Int J Radiat Biol.* 2022;98(9):1473–1483.
65. Wang N, Li F, du J, Hao J, Wang X, Hou Y, Luo Z. Quercetin protects against global cerebral ischemia-reperfusion injury by inhibiting microglial activation and polarization. *J Inflamm Res.* 2024;Volume 17:1281–1293.
66. Belfiore E, di Prima G, Angellotti G, Panzarella V, de Caro V. Plant-derived polyphenols to prevent and treat oral Mucositis induced by chemo-and radiotherapy in head and neck cancers management. *Cancers.* 2024;16(2):260.
67. Salama YA, el-karef A, el Gayyar AM, Abdel-Rahman N. Beyond its antioxidant properties: quercetin targets multiple signalling pathways in hepatocellular carcinoma in rats. *Life Sci.* 2019;236:116933.